Biomaterials 32 (2011) 57–64

Contents lists available at ScienceDirect

Biomaterials

journal homepage: www.elsevier.com/locate/biomaterials

Differentiation of neural stem cells in three-dimensional growth factor-immobilized chitosan hydrogel scaffolds

Nic D. Leipzig [a,b], Ryan G. Wylie [c], Howard Kim [d], Molly S. Shoichet [a,c,d,*]

[a] Department of Chemical Engineering and Applied Chemistry, University of Toronto, Toronto, Ontario, Canada
[b] Department of Chemical and Biomolecular Engineering, University of Akron, Akron, OH, USA
[c] Department of Chemistry, University of Toronto, Toronto, ON, Canada
[d] Institute of Medical Sciences, Toronto, ON, Canada

ARTICLE INFO

Article history:
Received 30 August 2010
Accepted 14 September 2010
Available online 8 October 2010

Keywords:
Neural stem cells
Hydrogel scaffolds
Chitosan
Neurons
Neurogenesis
IFN-gamma

ABSTRACT

The adult central nervous system (CNS) contains adult neural stem/progenitor cells (NSPCs) that possess the ability to differentiate into the primary cell types found in the CNS and to regenerate lost or damaged tissue. The ability to specifically and spatially control differentiation is vital to enable cell-based CNS regenerative strategies. Here we describe the development of a protein-biomaterial system that allows rapid, stable and homogenous linking of a growth factor to a photocrosslinkable material. A bioactive recombinant fusion protein incorporating pro-neural rat interferon-γ (rIFN-γ) and the AviTag for biotinylation was successfully expressed in *Escherichia coli* and purified. The photocrosslinkable biopolymer, methacrylamide chitosan (MAC), was thiolated, allowing conjugation of maleimide–strepatavidin via Michael-type addition. We demonstrated that biotin–rIFN-γ binds specifically to MAC-streptavidin in stoichiometric yields at 100 and 200 ng/mL in photocrosslinked hydrogels. For cell studies, NSPCs were photo-encapsulated in 100 ng/mL biotin–rIFN-γ immobilized MAC based scaffolds and compared to similar NSPC-seeded scaffolds combining 100 ng/mL soluble biotin–rIFN-γ vs. no growth factor. Cells were cultured for 8 days after which differentiation was assayed using immunohistochemistry for lineage specific markers. Quantification showed that immobilized biotin-rIFN-γ promoted neuronal differentiation (72.8 ± 16.0%) similar to soluble biotin–rIFN-γ (71.8 ± 13.2%). The percentage of nestin-positive (stem/progenitor) cells as well as RIP-positive (oligodendrocyte) cells were significantly higher in scaffolds with soluble vs. immobilized biotin–rIFN-γ suggesting that 3-D immobilization results in a more committed lineage specification.

1. Introduction

Recent advances in nanotechnology and tissue engineering afford exciting new regenerative medicine strategies. The principal goal of regenerative medicine is to promote tissue regeneration and healing after injury or disease [1]. This can be achieved through the delivery of cells and/or factors in a polymeric scaffold designed to provide a biomimetic microenvironment conducive to cell adhesion, proliferation, differentiation and host tissue integration. Thus far, the major hurdle for tissue engineering is to create 3-D microenvironments that provide the multiple synergistic stimuli necessary to predictably guide cell behavior. This is especially true for scaffolds incorporating cells created for central nervous system (CNS) regeneration where physicochemical signals are vital for survival and proper cell function.

Currently available clinical treatments for diseased or damaged CNS tissue provide only minor pharmacological relief and sometimes minimize further degeneration [2,3]. One of the central foci of functional repair after spinal cord injury, for example, is aimed at restoring active connections between neurons, allowing the return of motor and sensory function. Current research is investigating how neural stem/progenitor cells (NSPCs) can be utilized for functional tissue engineering as a potential treatment for neurodegenerative diseases, stroke, traumatic brain injury and spinal cord injury [4,5]. Stem cell therapy offers an attractive area of research for potential medical therapies, especially for treating injuries in the CNS. To successfully utilize stem cells, we must be able to influence their migration, proliferation and phenotype in a predictable manner. Currently, soluble biochemicals have proved most successful in altering NSPC function; however, this strategy is difficult to apply *in vivo* because of complexities involved in

* Corresponding author. University of Toronto, 160 College Street, Room 514, Toronto, ON, Canada M5S 3E1. Tel.: +1 416 978 1460; fax: +1 416 978 4317.
E-mail address: molly.shoichet@utoronto.ca (M.S. Shoichet).

0142-9612/$ – see front matter © 2010 Elsevier Ltd. All rights reserved.
doi:10.1016/j.biomaterials.2010.09.031

spatially controlling dosing locale, maintaining constant concentration over time and mitigating cost. Most importantly, the ability to implicitly influence a specific phenotype through physical stimuli has not yet been discovered [6]. NSPCs are defined by their ability to self-renew through mitotic cell division and differentiate into astrocytes, oligodendrocytes and neurons [7–9]. These stem cells exist in specialized microenvironments or niches in the mammalian brain and are able to generate a limited number of neurons and glia [10,11]. The physicochemical cues NSPCs require for proliferation, migration and differentiation are beginning to be understood [12]; however, significant work remains in terms of their incorporation into 3-D scaffolds for regenerative strategies.

The role of soluble factors in guiding stem cell function, such as self-renewal and fate decision, has been widely studied [7,13–22]. As a result, we have a nascent understanding of the ligands and signal transduction pathways that are used for self-renewal and differentiation. We have previously identified interferon-γ (IFN-γ) as a cytokine that favors differentiation of NSPCs into neurons [22,23]. Recent work has begun to reveal how covalent immobilization of growth factors/cytokines modifies cell and stem cell function [23–31]. Chemical immobilization of cytokines to biomaterial substrates allows for spatial control of differentiation with sustained dosing, which is not possible with soluble factors [24,28]. At the same time, cytokine immobilization allows the role of cellular internalization signal transduction to be studied [31]. We have recently shown that IFN-γ can be immobilized to the surface of a hydrogel scaffold to guide the differentiation of NSPCs preferentially to neurons [23]; however, the carbodiimide chemistry used to immobilize the protein was non-specific and inefficient. To overcome this limitation, we took advantage of the well-known (and strong) physical interaction between biotin and streptavidin such that biotin–rIFN-γ was expressed and streptavidin-modified hydrogels were synthesized.

Given the importance of the stem cell niche to define cell fate, the main objective of this study was to study the differentiation of NSPCs in a defined three-dimensional microenvironment. We hypothesized that recombinant biotin–rIFN-γ will enable immobilization to MAC-streptavidin and the creation of 3-D photocrosslinked scaffolds will preferentially stimulate differentiation of NSPCs to neurons. To this end, photocrosslinked methacrylamide-chitosan (MAC) hydrogel scaffolds were synthesized with both cell-adhesive GRGDS peptides and pro-neurogenic rIFN-γ immobilized to them and tested with NSPCs.

2. Materials and methods

2.1. Recombinant AviTag–IFN-γ cloning and expression

The protein sequence for IFN-γ was obtained from the NCBI and a fusion protein was designed incorporating a 6X histidine and biotin tag (AviTag) [32] to the N-terminus of the growth factor to enable Ni–NTA affinity purification and biotin labeling, respectively (Supplementary Table 1). A flexible hinge derived from the murine IgG3 hinge region [33] was incorporated between the AviTag and IFN-γ. These sequences were optimized for expression by *E. coli* and inserted into an isopropyl β-D-1-thiogalactopyranoside (IPTG; Bioshop, Burlington, ON Canada) inducible pET 21a(+) vector (DNA synthesis and cloning performed by GenScript, New Jersey, USA). BL21 (DE3) *E. coli* (New England Biolabs, Ipswich, MA, USA) were transformed with the recombinant vector. For recombinant protein expression, 1.8 L cultures of *E. coli* were grown in 47.6 g/L Terrific Broth, 4 mL/L glycerol and 100 μg/mL ampicillin (Bioshop) at 37 °C with air sparging to an optical density of 0.8. Expression was induced with the addition of 190 μg/mL IPTG. After 4 h, the cells were harvested and the expression of recombinant protein was assayed by sodium dodecyl sulfate polyacrylamide gel (SDS-PAGE) electrophoresis.

Soluble and insoluble (whole cell) protein fractions were prepared for SDS-PAGE. Soluble samples were prepared by pelleting 1 mL of the main culture, treating with 200 μL Bugbuster (Novagen, Darmstadt, Germany) for 30 min at room temperature (RT), followed by centrifugation (Beckman Microfuge 16; 15,000 g, 5 min, RT). 50 μL of the liquid phase was then transferred to a new tube and 50 μL of loading dye (Tris-SDS, glycerol, SDS, β-mercaptoethanol, Coomassie blue; Bioshop) was added and the samples were boiled for 5 min. Insoluble samples were prepared by pelleting 500 μL of the main culture, then adding 200 μL of loading dye followed by boiling for 5 min. These protein samples were run on 12% polyacrylamide tris (hydroxymethyl)aminomethane (Tris) HCl gels using the Invitrogen Xcell system (Carlsbad, CA, USA), stained with SimplyBlue SafeStain (Invitrogen), washed and imaged.

2.2. AviTag recombinant IFN-γ purification, renaturation and biotynilation

Harvested *E. coli* were centrifuged (Beckman Avanti J-26 XPI, rotor JLA 8.1; 15,000 g, 30 min, 4 °C) and the pellet was resuspended in denaturation buffer (6 M GuanidineHCl, 100 mM NaH_2PO_4, 10 mM Tris, 10 mM imidazole, pH 8.0; Bioshop) and rocked overnight at RT. The resulting mixture was centrifuged (Beckman Avanti J-26 XPI, rotor JA 25.50; 20,000 g, 15 min, RT) and the liquid fraction was incubated with 2 mL of nickel-nitrilotriacetic acid (Ni–NTA) resin solution (Qiagen, Valencia, CA, USA) at RT for 15 min then loaded into a chromatography column. Four washes were performed with 20 mL of denaturation buffer followed by elution two times with 15 mL of elution buffer (6 M GuanidineHCl, 200 mM glacial acetic acid).

For renaturation the resulting protein solution was placed in 1000 Da MWCO dialysis membranes (SpectraPor; Spectrum Labs, Rancho Dominguez, CA, USA). Recombinant AviTag–IFN-γ was first dialyzed against 0.02 M TrisBase, 0.15 M NaCl, 0.2 M GuanadineHCl, 0.5 M arginine at pH = 7.5 (Bioshop) overnight at RT followed by dialysis against 0.05 M TrisBase, 0.15 M NaCl pH = 7.5 for 4 h at RT. The solution was then concentrated (5000 MWCO; GE Healthcare, Piscataway, NJ, USA) to 2–3 mL for fast protein liquid chromatography (FPLC) purification (AKTA Explorer 10 with Frac-950 fraction collector, Amersham Pharmacia). AviTag–rIFN-γ was FPLC purified using the final dialysis buffer at 4 °C. After FPLC, the appropriate fractions, as detected by 280 nm absorbance, were collected and concentrated to 1–2 mL (5000 MWCO; GE). The resulting recombinant purified protein was assayed with matrix-assisted laser desorption/ionization time-of-flight mass spectrometry (MALDI-TOF) to confirm molecular weight. The final protein concentration was determined via absorbance measurement at 280 nm with a NanoDrop ND-100 UV spectrophotometer (Thermo Scientific, Waltham, MA) and calculated using an extinction coefficient of 19630 M^{-1} cm^{-1}.

To facilitate immobilization via biotin–streptavidin coupling, AviTag–rIFN-γ was biotinylated with biotin–protein ligase BirA500 (Avidity, Aurora, CA, USA) following the manufacturer's suggested procedures. For purification the reaction mixture was placed in a dialysis cartridge (10,000 MWCO; Thermo-Fisher, Pittsburgh, PA, USA) and dialyzed against PBS for 2 d with 3 changes per d. Biotinylation was quantified using the FluoReporter Biotin Quantitation assay kit (Invitrogen).

2.3. Recombinant biotinylated IFN-γ bioactivity

Bioactivity was tested *in vitro* by assaying the differentiation response of rat brain derived neural stem cells to sterile-filtered (0.2 μm) biotin–rIFN-γ and compared to commercially available rIFN-γ (Peprotech Inc., Rocky Hill, NJ, USA). NSPCs were isolated from the subependymal region of the lateral ventricles from the forebrain of adult female Wistar rats and expanded in neurosphere culture as explained previously [34]. Passage five neurospheres were dissociated into single cells and plated on the surface of poly-D-lysine (Sigma)/laminin (Invitrogen) coated glass coverslips at 37 °C and 5% CO_2 and cultured for 18 h in growth medium consisting of neurobasal media (NBM), 2 mM L-glutamine, 100 μg/mL penicillin–streptomycin, B27 (Invitrogen), 20 ng/mL epidermal growth factor (EGF-recombinant human, Invitrogen), 20 ng/mL basic fibroblast growth factor (bFGF-recombinant human, Invitrogen) and 2 μg/mL heparin (Sigma). The growth media was removed and replaced with differentiation medium (NBM, L-glutamine, penicillin–streptomycin, B27) and two growth factor treatments: 100 ng/mL biotin–rIFN-γ, 100 ng/mL commercial rIFN-γ. We have previously demonstrated that these concentrations are in the saturation range for IFN-γ mediated neuronal differentiation [23]. Cells were cultured in differentiation conditions for an additional 7 d, then fixed with 4% paraformaldehyde for 15 min. Bioactivity of biotin–rIFN-γ was confirmed by determining the percentage of cells positive for βIII-tubulin after immunohistochemistry (IHC) as described later.

2.4. Methacrylamide-chitosan synthesis and modification for protein coupling

MAC was synthesized and modified to enable immobilization of biotin–rIFN-γ as summarized in Fig. 1. MAC was synthesized with 23% methacryl substitution of chitosan (Protosan UP B 80/20, NovaMatrix, Drammen, Norway), as described previously [35]. Sulfhydryl side groups were added to MAC by way of Traut's reagent (2-iminothiolane; Toronto Research Chemicals Inc., Toronto, ON, Canada). For this reaction, MAC was first dissolved in distilled and deionized water (ddH_2O; Millipore Milli-RO 10 Plus and Milli-Q UF Plus system at 18 MΩ resistance; Billerica, MA, USA) at 2 wt% m/v. For the reaction, an equal volume of 0.2 M borate buffer (pH 8.0; Sigma) with 0.5 M 2-iminothiolane was added and the vial was mixed and left for 4 h on a shaker at RT. The solution was then placed in a dialysis membrane (12,000–14,000 MWCO; SpectraPor) and dialyzed against distilled water for 2 d with 3 changes per d then lyophilized. Ellman's reagent (5,5′-dithiobis-(2-nitrobenzoic acid); Sigma) was used to determine the amount of sulfhydryl modification

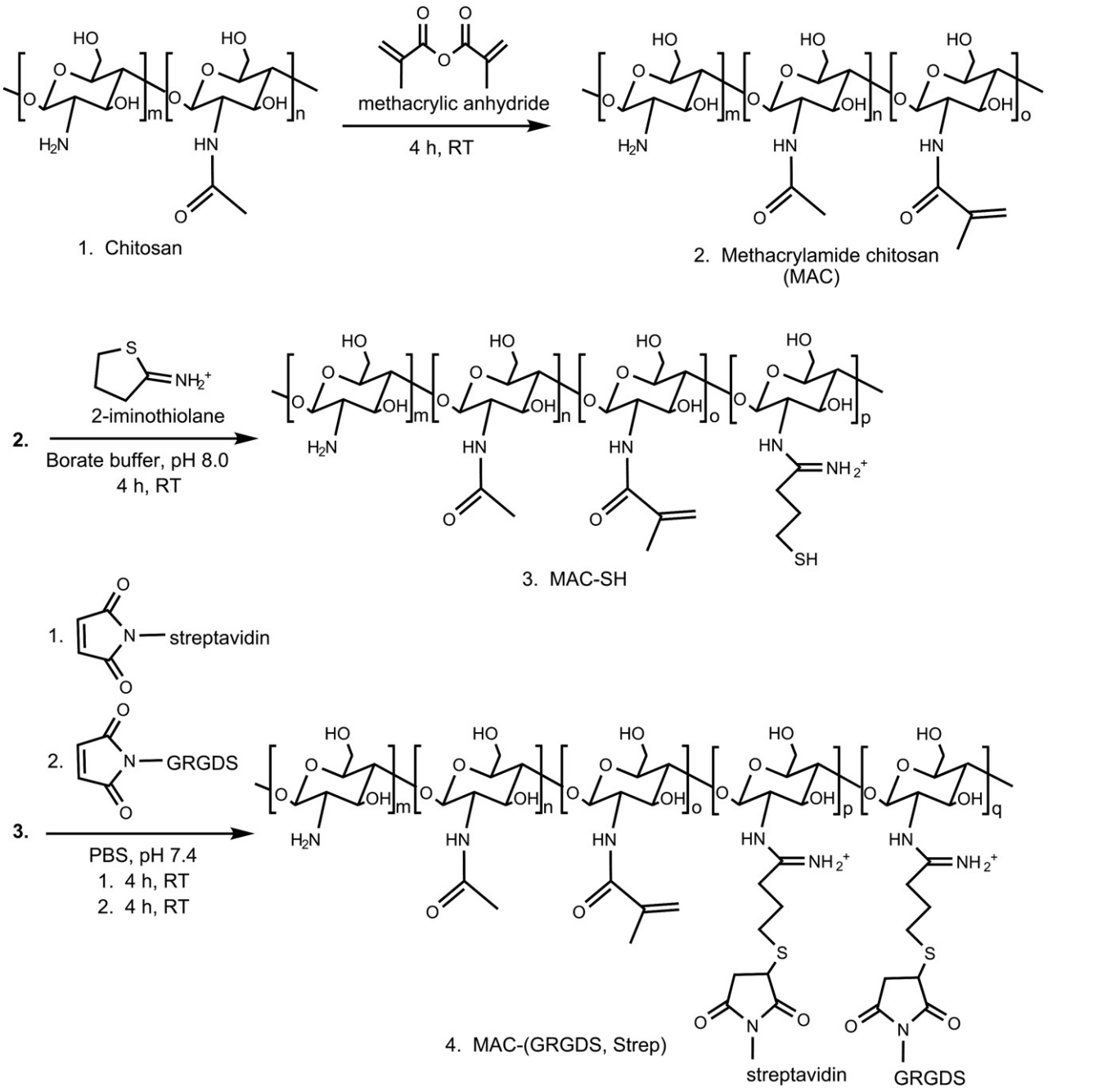

Fig. 1. Three step reaction scheme for creating MAC-(GRGDS, Streptavidin).

using an absorbance measurement at 412 nm and comparing it to a calibration curve of serially diluted cysteine standards (Sigma).

Next, lyophilized sulfhydryl-MAC was dissolved in PBS (pH 7.4) at 3 wt% m/v with 20 mM tris-(2-carboxyethyl)-phosphine hydrochloride (TCEP; Sigma). 10 μM maleimide-streptavidin (Sigma) was added and allowed to react by shaking overnight RT. 10 mM maleimide-GRDGS or maleimide-K(FAM)GRGDS (AnaSpec, San Jose, CA, USA) was next added and allowed to react by shaking overnight RT. The resulting mixtures were then placed in dialysis membranes (12,000–14,000 MWCO; SpectraPor) and dialyzed against PBS for 3-D with 3 changes per d. The amount of immobilized K(FAM)GRGDS was determined by fluorescent measurement (485 nm excitation, 520 nm emission) with comparison to a standard curve of maleimide-K(FAM)GRGDS.

2.5. Biotin–rIFN-γ immobilization

For quantification of protein immobilization, biotinylated rIFN-γ was fluorescently labeled with 5(6)-carboxyfluorescein, succinimidyl ester (5(6)-FAM, SE; Biotium, Hayward, CA, USA). Labeling was performed by adding thirty times molar excess of 5(6) FAM-SE and allowing the reaction to mix for 4 h. The reaction mixture was placed in a dialysis cartridge (10,000 MWCO; Thermo-Fisher) and dialyzed against PBS for 2 d with 3 changes per d. Protein concentration was determined via absorbance measurement after dialysis was completed.

Immobilization to modified MAC was carried out by adding the desired concentration of biotin–rIFN-γ and mixing for 4 h to allow binding to MAC-streptavidin. For quantification experiments, fluorescent biotin–rIFN-γ was mixed with 1 wt% streptavidin conjugated MAC in PBS to achieve final concentrations of 50, 100 and 200 ng/mL of biotin–rIFN-γ. A control for non-specific adsorption was included by reacting MAC-SH (no streptavidin) with 200 ng/mL fluorescent biotin–rIFN-γ. Hydrogel scaffolds were formed by adding the photoinitiator 1-hydroxycyclohexyl phenyl ketone (IRG-184; Sigma) dissolved into 100% ethanol at 300 mg IRG-184 per mL ethanol. The photoinitiator solution was sterile-filtered through a 0.2 μm filter, added to the MAC solutions at a concentration of 1.5 μl IRG-184 per g MAC and mixed/deaerated (SpeedMixer DAC 150 FVZ; Hauschild Engineering, Hamm, Germany). 100 μl of the resulting mixture was transferred to a 96-well plate and crosslinked for 2 min by UV light (365 nm) exposure. The resulting gels were washed

3 times per d for 3 d with PBS to remove unbound protein. Mechanical testing of the hydrogels (Mach-1 micromechanical testing system, BioSyntech, Laval, QC, Canada) yielded a Young's modulus (E_Y) of 0.77 ± 0.18 kPa which is similar to our previous studies [6,23] and native brain tissue [36,37].

2.6. NSPC 3-D culture in immobilized rIFN-γ methacrylamide-chitosan hydrogels

Cell culture experimentation was performed similarly to above. MAC-(streptavidin, GRGDS) in PBS was first sterilized by UV light for 2 h then solutions were made incorporating final concentrations of 100 ng/mL biotin–rIFN-γ (immobilized group), 100 ng/mL biotin–rIFN-γ (soluble group) and blank controls (control group). 2×10^6 cells/mL passage five dissociated NSPCs in growth medium and 1.5 μl IRG-184 solution per g total mass of solution were added to each group to achieve a final 1 wt% hydrogel scaffold (g modified MAC per total g solution). Each solution was mixed/deaerated before 100 μL was transferred into a 96-well plate and photo-crosslinked into hydrogel scaffolds with 2 min UV exposure. The remainder of each well was filled with growth medium. After 18 h, growth medium was replaced with minimum medium containing NBM, L-glutamine, penicillin–streptomycin, B27 (soluble group received 100 ng/mL biotin–rIFN-γ) and samples were cultured (37 °C, 5% CO_2) for an additional 7 d with media changes every 2 d. At the end of the culture period, samples were washed in PBS and fixed in 100% methanol at −20 °C for 15 min. Scaffolds were embedded and cryosectioned at 10 μm (Leica CM 3050S; Bannockburn, IL, USA) and mounted on glass slides.

2.7. Immunohistochemistry

The following primary antibodies were used for IHC: monoclonal mouse anti-β-III tubulin (1:1000; Covance, Princeton, New Jersey, USA) for neurons; monoclonal anti-RIP (1:5; Developmental Studies Hybridoma Bank, Iowa City, IA, USA) for oligodendrocytes; and monoclonal mouse anti-glial fibrillary acidic protein (GFAP, 1:100; Cell Sciences, Canton, MA, USA) for astrocytes and monoclonal mouse anti-nestin (1:500; BD Biosciences, San Jose, CA, USA). For all IHC procedures, appropriate controls were obtained by omission of the relevant primary antibody. Cell membranes were permeabilized with 0.1% Triton X-100 in PBS for 10 min (for paraformaldehyde fixed cells), washed 3 times then blocked with a solution of 10% FBS in PBS at room temperature for 1 h. Next, each primary antibody solution was added for 24 h at 4 °C. After washing with PBS 3 times, samples were exposed to secondary goat anti-mouse IgG Alexa-Fluor 546 (1:400; Invitrogen) for 2 h at room temperature and then washed with PBS buffer 3 times. Finally, cell nuclei were counterstained with 10 μM Hoechst 33342 (Invitrogen) for 7 min, washed with PBS buffer and mounted/coverslipped using ProLong Gold anti-fade reagent (Invitrogen).

2.8. Statistics

All statistical analyses were performed using JMP IN 7.1 (SAS Institute, Cary, NC, USA). Differences among groups were assessed by ANOVA with Tukey's *post-hoc* analysis to identify statistical differences among three or more treatments. All data are presented as mean ± SD.

3. Results

3.1. Recombinant protein expression, characterization and bioactivity

In this study, BL21(DE3) *E. coli* were transformed with the AviTag–IFN-γ pET 21a(+) plasmid and 4 h of IPTG induced production were sufficient to generate enough fusion protein for all experiments. Protein electrophoresis by SDS-PAGE (Fig. 2A) demonstrated that the expressed AviTag-rIFN-γ protein primarily resided in the insoluble fraction (inclusion bodies) of the BL21 (DE3) *E. coli* main culture. To obtain AviTag–rIFN-γ, the harvested *E. coli* pellet was completely denatured then purified utilizing the N-terminal 6X histidine tag. Optimally, 2 mL of Ni–NTA resin should yield a total of 80–100 mg of denatured protein according to the manufacturer's specifications. Since only a few mg were required for experimentation, renaturation (or refolding) by dialysis was used to generate the native structure. Renaturation was initially performed by

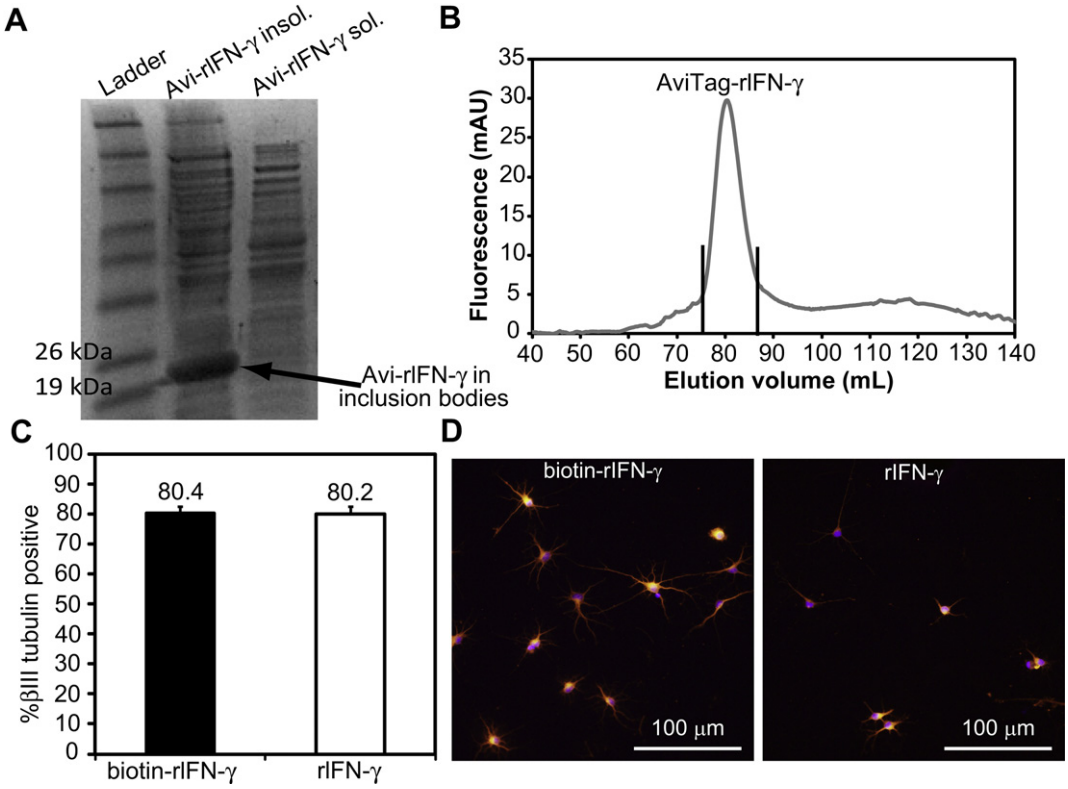

Fig. 2. Recombinant production, purification and bioactivity of rat biotin tagged IFN-γ. (A) SDS-PAGE protein electrophoresis of insoluble (Avi–rIFN-γ insol.) and soluble (Avi–rIFN-γ sol.) fractions of *E. coli* cultures expressing AviTag–rIFN-γ. (B) FPLC with Superdex 200 results in one main peak that was selected for downstream use. (C) Bioactivity was assayed after biotinylation/purification with NSPCs seeded onto laminin-coated glass coverslips given 100 ng/mL of both soluble biotin–rIFN-γ and commercial rIFN-γ. After 8 d cells were fixed and stained for the neuronal marker βIII tubulin and the number of positive cells were quantified. No significant difference in neuronal differentiation was observed ($p = 0.94$). Data are presented as mean ± SD, $n = 3$. (D) Representative fluorescence images of βIII tubulin and Hoechst 33342 staining are shown.

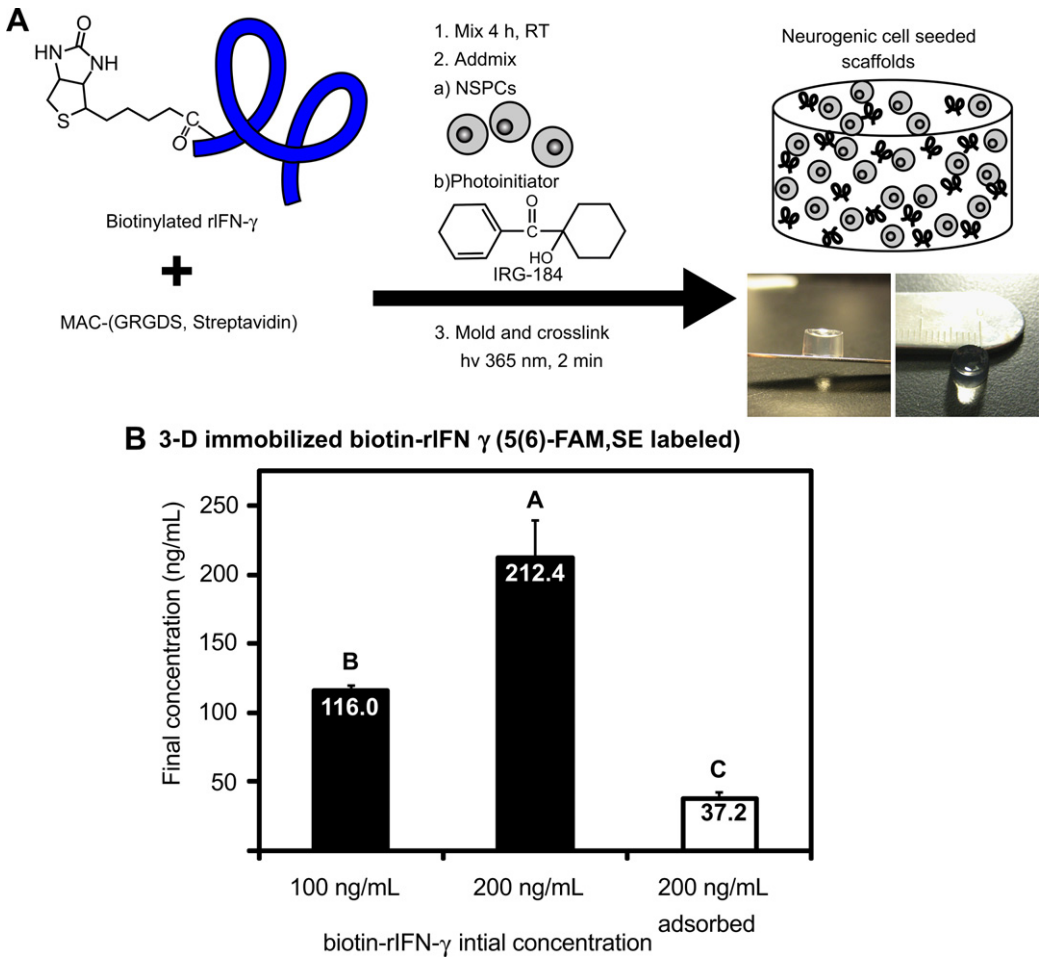

Fig. 3. Immobilization of biotin–rIFN-γ to MAC. (A) Biotin–rIFN-γ is immobilized to MAC-(GRGDS, Streptavidin) through biotin–streptavidin interaction. Cell seeded scaffolds are prepared by mixing cells and photoinitiator followed by exposure to UV light resulting in photocrosslinked scaffolds. (B) 5(6)-FAM,SE labeling was used to determine immobilized and adsorbed biotin–rIFN-γ concentration based on the initial admixed concentration. Washing demonstrated that adsorbed biotin–rIFN-γ was mostly removed whereas streptavidin-linked biotin–rIFN-γ was stably immobilized. A significant decrease in protein concentration between immobilized and adsorbed was calculated ($p < 0.0001$). Data are presented as mean ± SD, $n = 4$. Different letters indicate significant differences of at least $p < 0.05$.

dialysis in a Tris buffer with 0.2 M guanidine buffered at pH 7.5, which is sufficiently below the estimated isoelectric point (pI) of the fusion protein, pI = 8.64. This resulted in a small 2.00 mg yield of renatured AviTag–rIFN-γ from a 1.8 L main culture. The addition of 0.5 M D-arginine to the dialysis buffer increased the renatured yield to 7.02 mg. As shown in Fig. 2B, FPLC purified samples resulted in a single large peak, demonstrating purity of the sample. MALDI-TOF of renatured and FPLC purified AviTag–rIFN-γ had a molar mass of 21.41 kDa, which is similar to the theoretical molar mass of 21.35 kDa (Supplementary Table 1 DNA sequence 5′3′ frame 1 translation).

The FlowReporter Biotin Quantitation assay determined that AviTag-rIFN-γ was successfully biotinylated by the BirA enzyme with 102.7 ± 3.7% of rIFN-γ containing biotin. While the average is slightly above 100%, small errors may be the result of dialysis, transfer and pipetting steps. Before covalent attachment to MAC, the bioactivity of biotin-rIFN-γ was tested using 2-D *in vitro* culture on laminin-coated glass coverslips and compared to a commercial rIFN-γ. We have previously shown that NSPCs robustly differentiate when exposed to 100 ng/mL of soluble rIFN-γ [22,23] on laminin-coated surfaces. IHC for βIII tubulin with positive cell counting demonstrated similar neuronal differentiation percentages for our *E. coli*-expressed rIFN-γ fusion protein and commercially available rIFN-γ (80.4 ± 2.4% vs. 80.2 ± 2.3% respectively; Fig. 2C, D; $p = 0.94$).

3.2. MAC modification and covalent protein attachment

Maleimide-sulfhydryl chemistry was selected to covalently attach streptavidin to MAC in an aqueous solution through stable thioether bond formation. To enable maleimide-sulfhydryl cross-linking, first sulfhydryl-MAC was synthesized via the reaction with 2-iminothiolane. After purification, Ellman's assay determined that 1 wt% MAC-SH contained 4.1 ± 0.2 mM sulfhydryl groups. Sufficient maleimide-streptavidin was covalently linked to 1 wt% MAC to allow for protein immobilization and the remainder of free sulfhydryl groups were reacted with excess maleimide-GRGDS peptide. The attachment of this peptide served to both provide attachment ligands for NSPCs and quench any previously unreacted sulfhydryls. RGD provides a native attachment ligand for differentiating NSPCs and is found in basement membrane proteins including laminin and fibronectin [1,38]. A substitute reaction with maleimide-K(FAM)GRGDS was performed to determine how much peptide was covalently attached to the material. Fluorescent measurement after purification showed that 1 wt% streptavidin-MAC-K(FAM)GRDGS contained 4.3 ± 0.3 mM peptide.

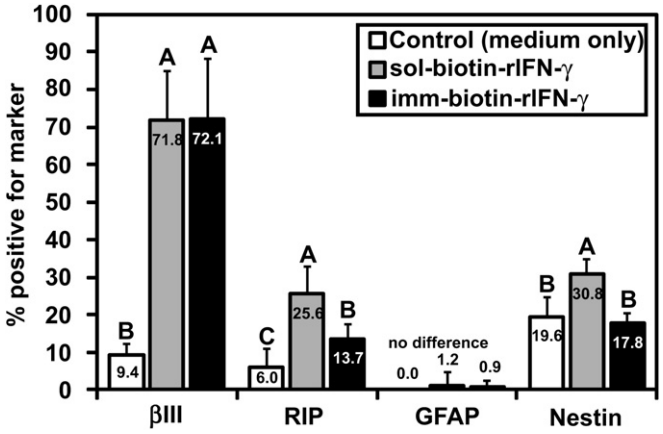

Fig. 4. Percentages of cells staining positive for βIII tubulin, RIP, GFAP and nestin in 3-D biotin–rIFN-γ immobilized and control MAC surfaces after 8 d in culture. Statistics were performed separately for each marker using one-way ANOVA with Tukey's *post-hoc* analysis; letters indicate significance ($p < 0.0001$). Neurons primarily resulted from 100 ng/mL soluble and immobilized biotin–rIFN-γ ($p < 0.0001$). A higher percentage of both RIP (oligodendrocytes, $p < 0.0001$) and nestin-positive (stem/progenitor, $p < 0.0001$) cells were found in scaffolds in the presence of soluble vs. immobilized biotin–rIFN-γ suggesting greater neuronal lineage commitment in scaffolds with immobilized biotin–rIFN-γ. Very little astrocyte differentiation was observed. Data are presented as mean ± SD, $n = 4$.

The presence of immobilized streptavidin on MAC-(GRGDS, Streptavidin) enables covalent attachment via biotinylated proteins in an aqueous solution and subsequent formation of scaffolds through photo-crosslinking of methacrylamide groups (Fig. 3A). Performing these procedures with biotinylated rIFN-γ demonstrates efficient binding to MAC-(GRGDS, Streptavidin) via admixing. Fluorescent assays revealed that all of the admixed biotin–rIFN-γ attached to the scaffold, whereas washing was able to remove 81.8 ± 2.4% of adsorbed biotin–rIFN-γ (i.e., when streptavidin was not conjugated to MAC prior to addition of biotin–rIFN-γ, Fig. 3B). This efficient coupling facilitated the synthesis of 3-D scaffolds with defined concentrations of IFN-γ.

3.3. Neural stem cell 3-D differentiation

Differentiation experiments with 3-D encapsulated NSPCs in MAC scaffolds and 100 ng/mL immobilized biotin–rIFN-γ were carried out for 8 d and compared to 100 ng/mL soluble biotin–rIFN-γ and medium without any growth factors (Figs. 4 and 5). IHC for neurons in scaffold cryosections revealed that immobilized biotin–rIFN-γ resulted in the same percentage of βIII+ neurons (72.8 ± 16.0%) as soluble biotin–rIFN-γ (71.8 ± 13.2%) after 8 d of culture ($p > 0.05$). The scaffold alone was insufficient to guide neuronal differentiation of encapsulated NSPCs with only 9.4 ± 2.8% of cells staining positive for the neuronal marker, βIII tubulin. Interestingly, in the presence of soluble biotin–rIFN-γ, significantly more RIP+ (oligodendrocytes) and nestin+ (stem/progenitor) cells were observed than in the presence of immobilized biotin–rIFN-γ and medium alone controls (Fig. 4, $p < 0.0001$). Significantly less nestin+ cells (17.8 ± 2.7%) were seen on immobilized scaffolds as compared to soluble treated scaffolds (30.8 ± 4.0%; $p < 0.0001$). Nestin staining can colocalize with βIII tubulin in semi-committed neuronal progenitors and immature neurons [39,40] thereby accounting for the greater than 100% of cell counts for the soluble biotin–rIFN-γ system. Considered together, these results suggest that immobilized IFN-γ results in a more neuronal committed population than soluble biotin–rIFN-γ, yet additional studies are required to probe this mechanism further. Very little GFAP positive staining was observed, which is consistent with previous studies using rat SVZ derived NSPCs [6,22,23].

4. Discussion

Photopolymerizable MAC offers a flexible platform for cells by allowing the incorporation of similar physicochemical cues to those found in their native niche. Using MAC scaffolds, NSPCs were shown to require a scaffold substrate with stiffness (Young's elastic modulus) less than 1 kPa for neuronal differentiation [6]. Moreover, MAC scaffolds facilitated the covalent modification of IFN-γ to the surface (i.e., 2-D) of <1 kPa scaffolds to encourage further neuronal differentiation [23]. In this study we aimed to build upon these 2-D findings and guide neuronal differentiation of NSPCs in 3-D using a more elegant immobilization strategy as a way to achieve more efficient and specific protein coupling. This necessitated recombinant addition of biotin near the N-terminus of an IFN-γ fusion protein and covalent modification of streptavidin to MAC. By mixing NSPCs with biotin–rIFN-γ immobilized MAC hydrogels prior to photo-crosslinking, the differentiation profile was investigated in 3-D. Immobilization of growth factors is advantageous for implantation strategies where sustained and local differentiation

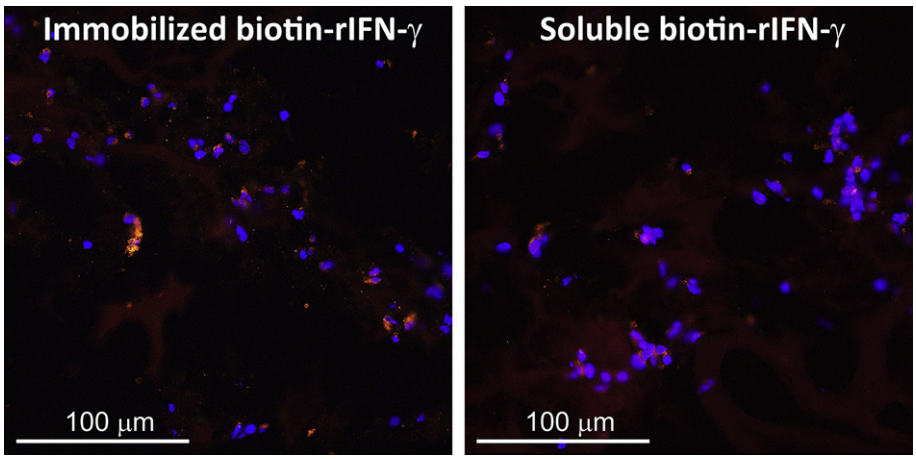

Fig. 5. Representative images of βIII tubulin IHC on 10 μm sections from biotin–rIFN-γ immobilized and soluble biotin–rIFN-γ treated 3-D MAC scaffolds after 8 d in culture. βIII tubulin (neurons) appears in red while the nucleus (Hoechst 33342) appears in blue.

are promoted in defined volumes of the biomaterial scaffold. Additionally, MAC provides a photocrosslinkable platform enabling molding, layering and/or the incorporation of biochemical gradients [41,42]. While MAC is enzymatically degraded by lysozyme, it did not degrade in the timeframe of the *in vitro* studies described herein [35].

This study demonstrates application of recombinant techniques to produce large quantities of an engineered fusion protein incorporating IFN-γ for specifying the 3-D differentiation of NSPCs into neurons. The fusion protein was produced first by designing a plasmid for *E. coli* expression that integrated a 6X histidine tag for Ni–NTA chromatography purification along with an AviTag sequence for site-specific biotinylation using the BirA enzyme (Supplementary Table 1). Despite insoluble protein expression in BL21(DE3), renaturation yielded ample milligram scale quantities of rIFN-γ fusion protein for all experiments. BirA completely biotinylated all protein as quantified by the FlowReporter Biotin Quantitation assay.

Recombinant technology offers the ability to engineer fusion proteins with nearly any desired functionalities. Fusion proteins are advantageous for protein immobilization because they provide control over protein binding and result in milligram scale (or higher depending on main culture or reactor size) quantities for downstream applications. Fusion proteins of growth factors and binding domains have been created previously to control immobilization to specific ECMs, biomaterials and cells. Fibronectin or fibronectin cell-binding domains have been incorporated in fusion proteins along with bFGF and EGF to stimulate vascularization and wound healing [43]. Collagen or collagen binding domains have also been incorporated into fusion proteins of bFGF [44], EGF [45,46], platelet derived growth factor (PDGF) [47], hepatocyte growth factor (HGF) [48] and nerve growth factor (NGF) [49] for targeted wound regeneration. Immobilization using these ECM binding mechanisms provides an equilibrium dissociation constant (K_d) for collagen binding on the order of 10^{-7} M [50] and on the order of 10^{-8} M for fibronectin [51]. The biotin–streptavidin immobilization used in this study uses a much stronger and more favorable biological association with a K_d on the order of 10^{-15} M [52]. Utilizing this binding mechanism allowed us to controllably and stably attach rIFN-γ containing fusion protein in solution to MAC (Fig. 3). This further facilitated the formation of pro-neurogenic NSPC-seeded 3-D scaffolds that encouraged significant neuronal differentiation after 8 d in basic medium containing no additional soluble growth factors (Figs. 4 and 5). This strategy would have been difficult and costly to perform without recombinantly produced AviTag–IFN-γ.

Synthesis of MAC-SH using Traut's reagent was selected for ease as well as coupling efficiency. This approach resulted in greater thiolation (4.1 mM for 1 wt% MAC) than we have reported previously using thioglycolic acid and carbodiimide coupling (0.996 mM for 2 wt% MAC) [35]. The addition of sulfhydryl groups to MAC facilitated the efficient and aqueous-based chemistry of both maleimide-streptavidin as well as maleimide-GRGDS. Sulfhydryl conjugation is advantageous since sulfhydryl occurrence in proteins or other biomolecules is usually low (2.26% of all amino acid residues found in mammals [53]), thus bioconjugation can be highly restricted [54]. The creation of a photocrosslinkable biopolymer incorporating rIFN-γ as a pro-neuronal differentiation factor, in addition to GRGDS as an attachment ligand, allowed for the creation of neurogenic 3-D scaffolds. Using these scaffolds, with only basic medium, we were able to guide NSPCs encapsulated within to primarily differentiate into neurons (Fig. 4). Similar results were seen in 3-D scaffolds in which cells were cultured in the presence of soluble biotin–rIFN-γ. βIII tubulin positive cells were seen evenly throughout both immobilized and soluble biotin–rIFN-γ scaffolds (Fig. 5). These results are an improvement over previous surface (2-D) immobilization data [23] where 60 ± 4% neurons were quantified on the highest IFN-γ surface concentration of 37.5 ng/cm^2. Not only did this study yield greater neuronal differentiation, we also were able to achieve complete/stoichiometric coupling of biotin–rIFN-γ to streptavidin-MAC whereas the immobilization on 2-D surfaces used carbodiimide chemistry that had a coupling efficiency of only 8.0 ± 0.6%.

In this study, a recombinant fusion protein incorporating a growth factor was shown to couple with 3-D biomaterial scaffolding through specific, favorable and strong binding in order to specify NSPC phenotype. Previous studies with growth factor fusion proteins have almost exclusively focused on incorporation of ECM binding domains for weaker non-specific binding [43–49]. In addition to guiding NSPC differentiation, 3-D immobilization of rIFN-γ could be advantageous for controlling the spatial differentiation/activation with sustained dosing of antigen-presenting cells (dendritic cells, macrophages and B lymphocytes), hematopoetic progenitor cells and T cells [55].

5. Conclusions

In this study, we show that the synthesis of photocrosslinkable streptavidin-modified MAC along with the recombinant production of biotin-IFN-γ facilitates the creation of 3-D hydrogels with immobilized IFN-γ. These scaffolds promote the differentiation of NSPCs into neurons in 3-D in the presence of only basic medium in one week. This approach enables creation of spatially tailored biomaterials for CNS regeneration while fostering further understanding of the basic principles influencing stem cell fate.

Acknowledgments

We are grateful to partial funding from NSERC (Discovery grant to MSS), Ontario Ministry of Research and Innovation postdoctoral fellowship (NDL), Fonds Québécois de la Recherche sur la Nature et les Technologies (FRQRNT) and Vision Science Research Program to RGW, Ontario Neurotrauma Foundation (HK) and the Advanced Food and Materials Network (AFM-Net to MSS). The authors would like to thank Dr. Tasneem Zahir for assistance with neural stem cell culture and assays, Dr. Ying Fang Chen for assistance with cell culture, Dr. Karen Maxwell for help and advice with recombinant protein production and Dr. Henry Krause for use of the AKTA FPLC.

Appendix. Supplementary data

Supplementary data associated with this article can be found, in the online version, at doi:10.1016/j.biomaterials.2010.09.031.

Appendix

Figures with essential color discrimination. Figs. 2, 3 and 5 in this article are difficult to interpret in black and white. The full color images can be found in the on-line version, at 10.1016/j.biomaterials.2010.09.031.

References

[1] Yu LMY, Leipzig ND, Shoichet MS. Promoting neuron adhesion and growth. Mater Today 2008;11:36–43.
[2] Orive G, Anitua E, Pedraz JL, Emerich DF. Biomaterials for promoting brain protection, repair and regeneration. Nat Rev Neurosci 2009;10:682–92.
[3] Straley KS, Foo CW, Heilshorn SC. Biomaterial design strategies for the treatment of spinal cord injuries. J Neurotrauma 2010;27:1–19.
[4] Walker PA, Aroom KR, Jimenez F, Shah SK, Harting MT, Gill BS, et al. Advances in progenitor cell therapy using scaffolding constructs for central nervous system injury. Stem Cell Rev 2009;5:283–300.

[5] Ayuso-Sacido A, Roy NS, Schwartz TH, Greenfield JP, Boockvar JA. Long-term expansion of adult human brain subventricular zone precursors. Neurosurgery 2008;62:223–9.
[6] Leipzig ND, Shoichet MS. The effect of substrate stiffness on adult neural stem cell behavior. Biomaterials 2009;30:6867–78.
[7] Cattaneo E, McKay R. Proliferation and differentiation of neuronal stem cells regulated by nerve growth factor. Nature 1990;347:762–5.
[8] Morshead CM, Reynolds BA, Craig CG, McBurney MW, Staines WA, Morassutti D, et al. Neural stem cells in the adult mammalian forebrain: a relatively quiescent subpopulation of subependymal cells. Neuron 1994;13:1071–82.
[9] Weiss S, Dunne C, Hewson J, Wohl C, Wheatley M, Peterson AC, et al. Multipotent CNS stem cells are present in the adult mammalian spinal cord and ventricular neuroaxis. J Neurosci 1996;16:7599–609.
[10] Gobbel GT, Choi SJ, Beier S, Niranjan A. Long-term cultivation of multipotential neural stem cells from adult rat subependyma. Brain Res 2003;980:221–32.
[11] Gotz M. Glial cells generate neurons–master control within CNS regions: developmental perspectives on neural stem cells. Neuroscientist 2003;9:379–97.
[12] Kazanis I. The subependymal zone neurogenic niche: a beating heart in the centre of the brain: how plastic is adult neurogenesis? Opportunities for therapy and questions to be addressed. Brain 2009;132:2909–21.
[13] Ahmed SRB, Weiss S. BDNF enhances the differentiation but not the survival of CNS stem cell-derived neuronal precursors. J Neurosci 1995;15:5765–78.
[14] Willerth SM, Sakiyama-Elbert SE. Approaches to neural tissue engineering using scaffolds for drug delivery. Adv Drug Deliv Rev 2007;59:325–38.
[15] Dhara SK, Stice SL. Neural differentiation of human embryonic stem cells. J Cell Biochem 2008;105:633–40.
[16] Benoit BO, Savarese T, Joly M, Engstrom CM, Pang L, Reilly J, et al. Neurotrophin channeling of neural progenitor cell differentiation. J Neurobiol 2001;46:265–80.
[17] Shetty AK, Turner DA. In vitro survival and differentiation of neurons derived from epidermal growth factor-responsive postnatal hippocampal stem cells: inducing effects of brain-derived neurotrophic factor. J Neurobiol 1998;35:395–425.
[18] Wong G, Goldshmit Y, Turnley AM. Interferon-gamma but not TNF alpha promotes neuronal differentiation and neurite outgrowth of murine adult neural stem cells. Exp Neurol 2004;187:171–7.
[19] Shingo T, Sorokan ST, Shimazaki T, Weiss S. Erythropoietin regulates the in vitro and in vivo production of neuronal progenitors by mammalian forebrain neural stem cells. J Neurosci 2001;21:9733–43.
[20] Nakayama T, Momoki-Soga T, Inoue N. Astrocyte-derived factors instruct differentiation of embryonic stem cells into neurons. Neurosci Res 2003;46:241–9.
[21] Kim SJ, Son TG, Kim K, Park HR, Mattson MP, Lee J. Interferon-gamma promotes differentiation of neural progenitor cells via the JNK pathway. Neurochem Res 2007;32:1399–406.
[22] Zahir T, Chen YF, Macdonald JF, Leipzig N, Tator CH, Shoichet MS. Neural stem/progenitor cells differentiate in vitro to neurons by the combined action of dibutyryl cAMP and interferon-gamma. Stem Cells Dev 2009;18:1423–32.
[23] Leipzig ND, Xu C, Zahir T, Shoichet MS. Functional immobilization of interferon-gamma induces neuronal differentiation of neural stem cells. J Biomed Mater Res A 2010;93:625–33.
[24] Kuhl PR, Griffith-Cima LG. Tethered epidermal growth factor as a paradigm for growth factor-induced stimulation from the solid phase. Nat Med 1996;2:1022–7.
[25] Kapur TA, Shoichet MS. Chemically-bound nerve growth factor for neural tissue engineering applications. J Biomater Sci Polym Ed 2003;14:383–94.
[26] Fan VH, Tamama K, Au A, Littrell R, Richardson LB, Wright JW, et al. Tethered epidermal growth factor provides a survival advantage to mesenchymal stem cells. Stem Cells 2007;25:1241–51.
[27] Nakajima M, Ishimuro T, Kato K, Ko IK, Hirata I, Arima Y, et al. Combinatorial protein display for the cell-based screening of biomaterials that direct neural stem cell differentiation. Biomaterials 2007;28:1048–60.
[28] Alberti K, Davey RE, Onishi K, George S, Salchert K, Seib FP, et al. Functional immobilization of signaling proteins enables control of stem cell fate. Nat Methods 2008;5:645–50.
[29] Aizawa Y, Leipzig N, Zahir T, Shoichet M. The effect of immobilized platelet derived growth factor AA on neural stem/progenitor cell differentiation on cell-adhesive hydrogels. Biomaterials 2008;29:4676–83.
[30] Shen YH, Shoichet MS, Radisic M. Vascular endothelial growth factor immobilized in collagen scaffold promotes penetration and proliferation of endothelial cells. Acta Biomater 2008;4:477–89.
[31] Wall ST, Saha K, Ashton RS, Kam KR, Schaffer DV, Healy KE. Multivalency of Sonic hedgehog conjugated to linear polymer chains modulates protein potency. Bioconjug Chem 2008;19:806–12.
[32] Tucker J, Grisshammer R. Purification of a rat neurotensin receptor expressed in *Escherichia coli*. Biochem J 1996;317(Pt 3):891–9.
[33] Deyev SM, Waibel R, Lebedenko EN, Schubiger AP, Pluckthun A. Design of multivalent complexes using the barnase*barstar module. Nat Biotechnol 2003;21:1486–92.
[34] Zahir T, Nomura H, Guo XD, Kim H, Tator C, Morshead C, et al. Bioengineering neural stem/progenitor cell-coated tubes for spinal cord injury repair. Cell Transpl 2008;17:245–54.
[35] Yu LM, Kazazian K, Shoichet MS. Peptide surface modification of methacrylamide chitosan for neural tissue engineering applications. J Biomed Mater Res A 2007;82:243–55.
[36] Taylor Z, Miller K. Reassessment of brain elasticity for analysis of biomechanisms of hydrocephalus. J Biomech 2004;37:1263–9.
[37] Gefen A, Margulies SS. Are *in vivo* and *in situ* brain tissues mechanically similar? J Biomech 2004;37:1339–52.
[38] Miner JH, Yurchenco PD. Laminin functions in tissue morphogenesis. Annu Rev Cell Dev Biol 2004;20:255–84.
[39] Mignone JL, Kukekov V, Chiang AS, Steindler D, Enikolopov G. Neural stem and progenitor cells in nestin-GFP transgenic mice. J Comp Neurol 2004;469:311–24.
[40] Encinas JM, Enikolopov G. Identifying and quantitating neural stem and progenitor cells in the adult brain. Methods Cell Biol 2008;85:243–72.
[41] Yu LM, Miller FD, Shoichet MS. The use of immobilized neurotrophins to support neuron survival and guide nerve fiber growth in compartmentalized chambers. Biomaterials 2010;31:6987–99.
[42] Aizawa Y, Wylie RG, Shoichet MS. Endothelial cell guidance in 3-D patterned scaffolds. Advanced Materials, in press, doi:10.1002/adma.201001855.
[43] Hashi H, Hatai M, Kimizuka F, Kato I, Yaoi Y. Angiogenic activity of a fusion protein of the cell-binding domain of fibronectin and basic fibroblast growth factor. Cell Struct Funct 1994;19:37–47.
[44] Andrades JA, Wu LT, Hall FL, Nimni ME, Becerra J. Engineering, expression, and renaturation of a collagen-targeted human bFGF fusion protein. Growth Factor 2001;18:261–75.
[45] Hayashi M, Tomita M, Yoshizato K. Production of EGF-collagen chimeric protein which shows the mitogenic activity. Biochim Biophys Acta 2001;1528:187–95.
[46] Nishi N, Matsushita O, Yuube K, Miyanaka H, Okabe A, Wada F. Collagen-binding growth factors: production and characterization of functional fusion proteins having a collagen-binding domain. Proc Natl Acad Sci USA 1998;95:7018–23.
[47] Lin H, Chen B, Sun W, Zhao W, Zhao Y, Dai J. The effect of collagen-targeting platelet-derived growth factor on cellularization and vascularization of collagen scaffolds. Biomaterials 2006;27:5708–14.
[48] Ota T, Gilbert TW, Schwartzman D, McTiernan CF, Kitajima T, Ito Y, et al. A fusion protein of hepatocyte growth factor enhances reconstruction of myocardium in a cardiac patch derived from porcine urinary bladder matrix. J Thorac Cardiovasc Surg 2008;136:1309–17.
[49] Sun W, Lin H, Chen B, Zhao W, Zhao Y, Dai J. Promotion of peripheral nerve growth by collagen scaffolds loaded with collagen-targeting human nerve growth factor-beta. J Biomed Mater Res A 2007;83:1054–61.
[50] Wang H, Fertala A, Ratner BD, Sage EH, Jiang S. Identifying the SPARC binding sites on collagen I and procollagen I by atomic force microscopy. Anal Chem 2005;77:6765–71.
[51] Zhang Z, Morla AO, Vuori K, Bauer JS, Juliano RL, Ruoslahti E. The alpha v beta 1 integrin functions as a fibronectin receptor but does not support fibronectin matrix assembly and cell migration on fibronectin. J Cell Biol 1993;122:235–42.
[52] Weber PC, Ohlendorf DH, Wendoloski JJ, Salemme FR. Structural origins of high-affinity biotin binding to streptavidin. Science 1989;243:85–8.
[53] Miseta A, Csutora P. Relationship between the occurrence of cysteine in proteins and the complexity of organisms. Mol Biol Evol 2000;17:1232–9.
[54] Hermanson GT. Bioconjugate techniques. San Diego: Academic Press; 1996.
[55] Young HA, Hardy KJ. Role of interferon-gamma in immune cell regulation. J Leukoc Biol 1995;58:373–81.